CHAPTER 5

To study the underlying molecular mechanisms regulating MeCP2 phosphorylation and its chromatin association

5.1 Introduction

In the previous chapter 4, the study mainly investigated the diverse developmental stimuli influencing the MeCP2 phosphorylation in glial cells and the data obtained demonstrated only few factors that influenced significantly the pMeCP2s expression and distribution patterns. In oligodendrocytes, among all the factors that were tested, ECM mainly Laminin (LN) showed a significant effect on MeCP2 S80 phosphorylation. However, in astrocytes and C6 glioma, BDNF showed a substantial effect on MeCP2 phosphorylation. Moreover, in LPS treated astrocytes there was significant increase in the MeCP2 S421phopshorylation. Therefore, in this chapter the molecular mechanisms the underlying this phosphorylation and its chromatin association were studied in detail.

Studies have reported that MeCP2 phosphorylation modulates the interaction of MeCP2 with chromatin (Bellini et al., 2014). Upon neuronal depolarization, S80 MeCP2 becomes dephosphorylated thereby allowing the MeCP2 to get dissociated from chromatin leading to gene expression (Gonzales et al., 2012). Recently, a study revealed that neuronal depolarization leads to the phosphorylation of MeCP2 at threonine 308 (T308) in the TRD domain of MeCP2 with the co-repressor NCoR complex (Ebert et al., 2013). Further, this study also reported that in MeCP2 T308A knock-in (KI) mice, there was significant reduction in neuronal activity-dependent induction of Npas4 and Bdnf mRNA because of the T308A mutation affected the chromatin architecture which leads to excitatory/inhibitory balance and indirectly reduces the levels of Npas4 and Bdnf mRNA (Ebert et al., 2013).In a general mechanism at the chromatin level, the neuronal depolarization leads to Ca2+ influx which activated the Cam kinases (CamkII) which in turn phosphorylates different substrates comprising MeCP2, CREB and H3S10 (Cortes et al., 2013). The phosphorylation at MeCP2 (S421) weakens its interaction with the chromatin which leads to chromatin relaxation which is due to CREB phosphorylation (Parker et al., 1996) which permits it to bind to CBP (CREB-binding protein a histone acetyl transferase) thereby leading to acetylation of histones (Ausio 2017).These modifications are helpful for the chromatin to be in a more open conformation which improves the availability of the transcriptional co-activators which leads to gene activation (Cortes et al., 2013; Flavell et al., 2008). However, till date there are no

reports on the MeCP2 phosphorylation and its chromatin association in glial cells of CNS. Over all, in this chapter the study is designed in such a way so as to elucidate the mechanisms underlying the stimuli dependent MeCP2 phosphorylation and its chromatin association. Data from the current proposed study will help us to better understand the tight regulation of glial MeCP2 phosphorylation sites which may function as a general regulatory switch that are made accessible to diverse stimuli acting through distinct signaling pathways with significant functional outcomes in different glial cell types that participates in diverse axo-glial interaction settings.

5.2 Plan of work

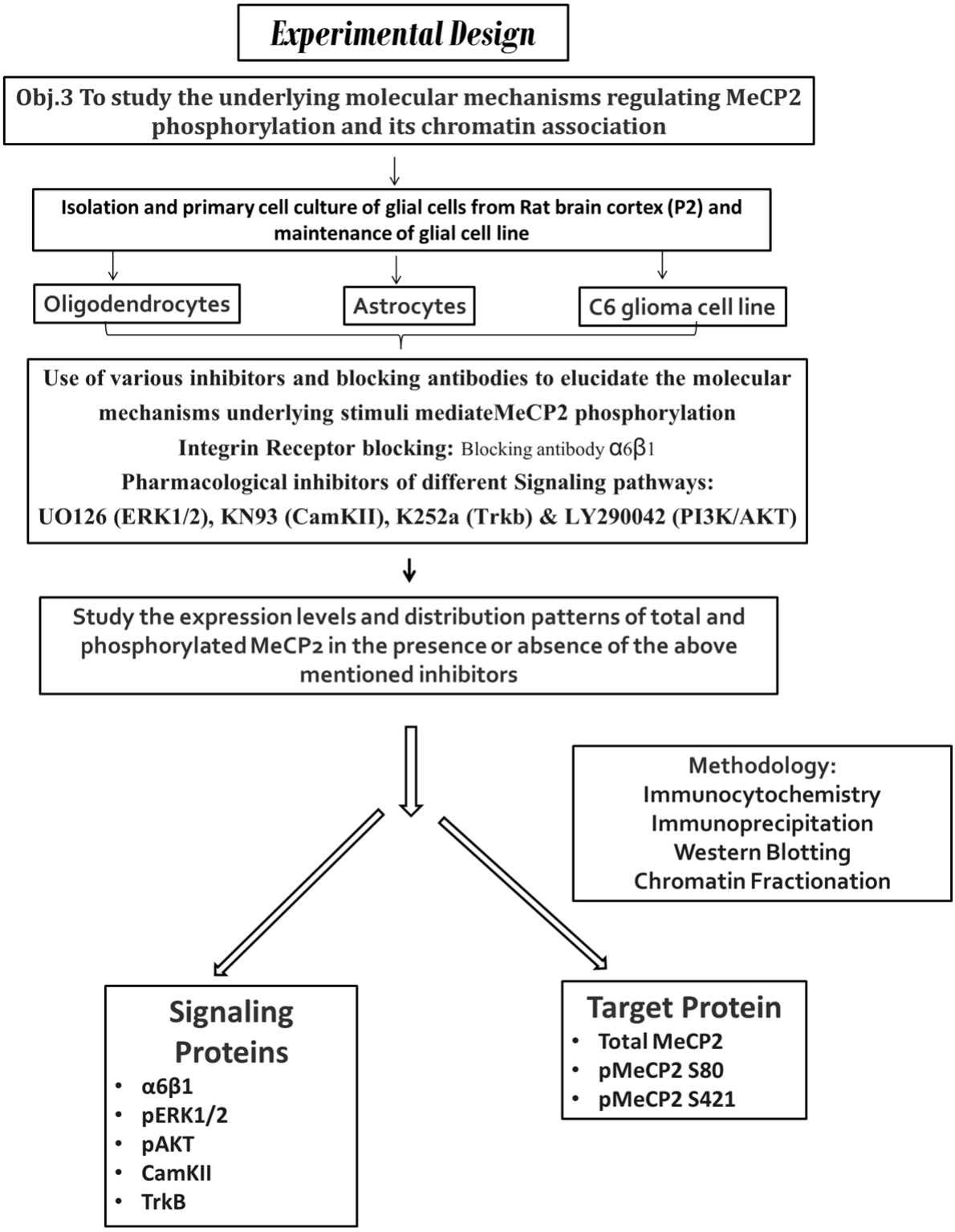

5.3 Results

5.3.1 Involvement of α6β1-integrinin the LN dependent MeCP2 dephosphorylation at S80 in OLGs

In chapter 4, it was shown that when mature OLGs were treated with LN there is significant decrease in pS80MeCP2 levels compared to the control treatment group. Hence to verify this observation, LN receptor, α6β1-integrin, which is the only known LN receptor (Baron et al. 2003) was pharmacologically blocked using appropriate blocking antibody. The expression of α6β1-integrin in immature and mature OLGs was confirmed using co-immunoprecipitation studies [Fig-5.1 (A)]. Then after, to verify the dephosphorylation of pS80MeCP2 mediated by LN receptor; the LN receptorα6β1-integrin was blocked using blocking antibody. Blocking α6β1 significantly increased the expression of pS80MeCP2 compared to LN [Fig-5.1 (B&C)].There was significant increase ($P<0.05$) in the pS80MeCP2 in the LN receptor blocking group compared to LN treated OLGs. Moreover, to study the nuclear localization and chromatin association of pS80MeCP2, immunocytochemistry was performed. The data indicated significant decrease in the LN-dependent nuclear pS80MeCP2 expression and co-localization as compared to the PLL control [Fig-5.1 (D-k)]. However, blocking the LN receptor (α6β1) significantly altered the LN-dependent decrease in the nuclear pS80MeCP2 expression and colocalization [Fig-5.1 (D-l)]. Nuclear co-localization and chromatin association were further confirmed by the study of the mean fluorescence intensity of the nuclear pMeCP2 in the LN and LN receptor blocking groups [Fig-5.1 (E)].This study suggests the importance of LN in regulating pS80MeCP2 in mature OLGs and thereby controlling the myelin gene expression.

5.3.2 CaMKII facilitates the BDNF stimulated phosphorylation of MeCP2 at S421 in astrocytes

In chapter 4, data showed significant increase in the levels of pS421MeCP2 in the BDNF treated astrocytes. Hence, the study was designed to investigate the pathways involved in the BDNF dependent MeCP2 S421 phosphorylation. Moreover, TrkB receptor is primarily activated by BDNF. MAPK, pAKT and pCamKII are shown to be involved in the TrkB signaling in astrocytes (Liu et al., 2017). Moreover, TrkB receptor is primarily involved in activating these signaling pathways. Hence, the levels of TrkB, pERK1/2,pAKT and CAMKII after BDNF exposure in astrocytes were analyzed. Phosphorylation of AKT, ERK1/2 and CamKII [Fig- 5.2(A)] were observed after 1hour exposure of BDNF in astrocytes. As shown in [Fig. 5.2 (A-D)], the levels of pERK1/2, pAKT and pCamKII were significantly increased in the BDNF treated astrocytes ($P<0.01$, $P<0.01$, $P<0.05$), compared with the control group. Moreover, data showed significant increase in the TrkB receptor levels in BDNF treated astrocytes compared to the control. To examine whether these pathways were involved in BDNF mediatedMeCP2 phosphorylation in astrocytes; specific pharmacological inhibitors were employed to inhibit respective signaling pathways. Following are the pharmacological inhibitors that were used in the present study: UO126 (10μM) for pERK1/2 (Jiang et al., 2002), LY290042 (50μM) for PI3K (Zhou et al., 2006), KN93 (5μM) for CamKII (Layton et al., 2004) and K252a (0.2μM) to inhibit TrkB receptor (Zhou et al., 2006). The astrocytes were treated with the above mentioned pharmacological inhibitors individually for 1hr prior to the treatment of BDNF followed by BDNF treatment for 1 hour. DMSO treatment group served as control. Treatment with KN93 resulted in an approximate 2 fold decrease ($P<0.01$) in the pS421MeCP2 levels compared to the BDNF treated group [5.2 (E, F)]. Moreover, there was significant decrease ($P<0.01$) in pS421MeCP2 expression in the K252 group which is the known inhibitor for TrkB receptor [5.2 (E, F)].Hence, these observations indicates, there is an involvement of CAMKII in BDNF mediated MeCP2 phosphorylation in astrocytes. However, there was no significant difference in the pS80MeCP2 expression in these inhibitor treated groups[5.2 (E, G)].

5.3.3 BDNF treatment results in the sub-cellular distribution of pS421MeCP2 in astrocytes

Next, the study examined pS421MeCP2 chromatin binding using immunocytochemistry following treatment of astrocytes with BDNF. As observed in chapter 4, thepS421MeCP2nuclear localization upon BDNF treatment hence, further localization of pS421MeCP2 and its chromatin association upon BDNF treatment in astrocytes and its expression in presence of CamKII inhibitor were analyzed.MeCP2 protein is known to be associated with the heterochromatin region of the DNA(Koch and Stratling, 2004). Rather, pS421MeCP2 is associated with activation of genes (Zhong et al., 2014) and based on this the distribution and chromatin association of pS421MeCP2 in the BDNF treated astrocytes using epifluorescence microscopy was further analyzed. Data indicated that on BDNF treatment the pS421MeCP2 was localized into the nuclei from the cytoplasm [5.3 (a, b)].Moreover, following immunocytochemistry, the sub-nuclear localization of pS421MeCP2 in the BDNF treated astrocytes were assessed and it was shown to be associated with the euchromatin region [5.3 (a, b)]. Whereas in the CamKII inhibited group there was decrease in the level of pS421MeCP2 and the association of pS421MeCP2 with the euchromatin also decreased drastically[5.3 (b, c)].This study suggests that pMeCP2S421 is redistributed in nucleus of astrocytes upon BDNF treatment and also associated with euchromatin which is regulated by CamkII pathway.

5.3.4 BDNF differentially regulates pMeCP2S80 and pMeCP2S421 expression in C6 glioma

To further study the effects of BDNF on MeCP2 phosphorylation and its chromatin association C6glioma cell line was used as a model system. In chapter 4, the effects of NGF and BDNF in the C6 glioma cell line were investigated and the data showed increase in MeCP2 phosphorylation. Hence, the underlying mechanism by which BDNF phosphorylates MeCP2 in glioma was further explored. In addition to this, the chromatin association of the phosphorylated MeCP2 induced by BDNF in C6 glioma cell line was

also analyzed. To explore the molecular mechanisms regulating MeCP2 phosphorylation in C6 glioma we checked the signaling pathways induced by BDNF in C6 glioma cells similar to that in astrocytes. The expression of pERK1/2, pAKT and pCamKII in BDNF treated C6 glioma cell line were analyzed and there was significant increase ($P<0.05$) in the expression of each of these signaling proteins compared to the control groups [Fig-5.4 (A-D)]. The expression of TrkB receptor was also as it is involved in activating these signaling pathways in glioma (Lawn et al., 2014). There was significant increase in the TrkB receptor expression in the BDNF treated C6 glioma cell line compared to the control group. Hence, further studies were carried out to examine the involvement of above mentioned pathways in BDNF mediated MeCP2 phosphorylation in C6 glioma cell line. For this, we used specific pharmacological inhibitors like UO126(10μM), LY290042(50μM), KN93(5μM) and K252a(0.2μM) to inhibit pERK1/2, pAKT, CamKII and TrkB receptor signaling respectively. The C6 glioma cell line was treated with the above mentioned inhibitors individually for 1hr prior to the treatment of 1 hour BDNF exposure. DMSO treatment group served as control. Data showed only K252 could significantly ($P<0.05$) impair the expression of MeCP2 phosphorylation at S80 as well as at S421 sites [Fig-5.4 (E-G)] whereas other inhibitors did not affect the levels of pS80MeCP2 and pS421MeCP2. The treatment with K252 resulted in an approximate 1.5 fold decrease in the pS421MeCP2 levels compared to the BDNF treated group [Fig-5.4 (E, F)]. Moreover, there was significant decrease ($P<0.05$) in pS80MeCP2 expression in the K252 group which is the known inhibitor for TrkB receptor [Fig-5.4 (E, G)]. This study indicates that none of these signaling pathways play a role in BDNF mediated MeCP2 phosphorylation. Moreover, BDNF stimulated the MeCP2 phosphorylation which is mediated by TrkB. However, the downstream signaling pathway do not involve either of pERK1/2, pAKT and CAMKII and hence the signaling pathway downstream of TrkB needs to be further explored

5.3.5 Differential chromatin binding of pS80 and pS421MeCP2 in BDNF treated C6 glioma cell line

Next, the study was planned to investigate the chromatin association of pS80MeCP2 and pS421MeCP2 in the BDNF treated C6 glioma cell line. To examine the sub-cellular localization and chromatin association, epifluorescence microscopy was employed. The BDNF treated C6 glioma cell line was stained with pS80 and pS421MeCP2 proteins individually and counterstained with DAPI to visualize the chromatin association. This was visualized using confocal laser scanning microscopy at 100X resolution. pS80MeCP2 staining in the BDNF treated C6 glioma was observed in the condensed region of DAPI positive nucleus which are referred as chromocenters [Fig 5.5 (A)] whereas pS421MeCP2 in the BDNF treated group did not co-localize with the chromocenters rather it was seen to be localized in the euchromatin region of the DAPI [Fig 5.5 (C)]. In order to report the amount of chromocenter grouping, the number of chromocenters in the cells expressing pS80MeCP2 proteins were quantified [Fig 5.5(B)]. Further, to compare the sub-nuclear localization of the BDNF induced MeCP2 phosphorylation, biochemical fractionation of nuclei was carried out (See chapter 2). Micrococcal nuclease fractionation of purified nuclei generates three distinct nuclear fractions, S1, S2, and P [Fig 5.6 (A)]. The S1 and P fractions primarily contain actively expressed genes and genes poised for expression, while the S2 fraction consists largely of constitutively silenced genes (Rose and Garrad 1984).The chromatin binding properties of MeCP2 probably depend on its affinity for nucleosomal and naked DNA. It was observed that the total MeCP2 was associated with the S1 fraction which is the nuclease-sensitive fraction enriched for actively expressed genes in the control as well as BDNF treated C6 glioma cell line [Fig 5.6 (B)].This is in agreement with recently published results from Good et al., 2017 and other reports showing that the majority of MeCP2is found in the S1 fraction (Thambirajahet al., 2012 & Gonzales et al., 2012).There was difference in the distribution of pS421MeCP2 and pS80MeCP2, pS421MeCP2 was found in the S1 fraction while pS80MeCP2 was found in the insoluble S2 fraction upon treatment with BDNF [Fig 5.6 (B)].Moreover, H3 (Histone 3) which is known to be associated with the inactive genes was found to be associated with the

insoluble S2 and P fractions. The data suggest that pS80MeCP2 gets associated with the insoluble fraction S2 and P upon treatment of BDNF while pS421MeCP2 is linked with the transcriptionally active S1 fraction which further indicates that pS80MeCP2 might play a role in transcription repression while pS421MeCP2 play a role in transcription activation.

5.3.6 LPS induced MeCP2 phosphorylation at S421 in astrocytes involves pERK1/2

To determine the molecular mechanisms involved in the LPS induced pS421MeCP2 expression, two pathways activated by LPS i.e PI3K and -pERK1/2 in astrocytes were analyzed (Gorina et al., 2010). There was significant increase in the levels of pAKT ($P<0.01$) and pERK1/2 ($P<0.01$) in the LPS treated astrocytes compared to the control groups [Fig-5.7 (A, B, C)]. Therefore, to study the involvement of these pathways in the LPS induced MeCP2 phosphorylation at S421 site we used specific inhibitors i.e UO126 and LY290042 to inhibit pERK1/2 and PI3K pathways respectively. Astrocytes were treated with pharmacological inhibitors for pERK1/2 and PI3K for a period of 2 hours and followed by treatment of LPS for 4hours.pS421MeCP2 levels were checked using western blotting. The results showed decrease in pS421MeCP2 in the UO126 treated group ($P<0.01$) compared to the LPS treated group [Fig-5.7 (D, E)]. However, there was no significant difference in the expression of pS421MeCP2 in LY290042 inhibitor group ($P>0.05$)[Fig-5.7 (D, E)].Moreover, to study the localization and chromatin association of pS421MeCP2, immunocytochemistry was performed. The data indicated significant increase in pS421MeCP2 in the LPS treated astrocytes which were mostly found to be localized in the cytoplasm region than nuclear compared to the control group [Fig-5.7 (F)]. However, by blocking the pERK1/2 pathway significantly decreased the LPS dependent increase in the cytoplasmic pS421MeCP2 expression [Fig-5.7 (F)]. Nuclear co-localization and chromatin association was further confirmed by the study of the mean fluorescence intensity of the nuclear pMeCP2 in the LPS and pERK1/2 inhibitor groups [Fig-5.7 (F)].

Discussion:

Oligodendrocyte development involves a large number of both intrinsic and extrinsic factors. OLG development is basically controlled by different transcription factors and chromatin remodeling through the extrinsic and intrinsic signaling molecules and neuronal activity (Zuchero and Barres, 2013). Oligodendrocyte differentiation process involves both the activation of genes that support differentiation, and repression of genes that inhibit differentiation (He and Lu, 2013). Hence, there is an excessive need to reveal the transcriptional regulators in OPCs/OLs which work together to precisely harmonize these cellular changes (Swiss et al., 2011). Moreover, in the last few years it has become clear that chromatin remodeling is a key process by which OLGs regulates its development (He and Lu 201; Emery et al., 2010; Jacob et al., 2011). A study demonstrated that Shh, which stimulates OLG differentiation, induces histone deacetylation by HDACs; whereas, inhibitory BMP4 seems to block the HDAC deacetylation (Wu et al., 2012). Major role of HDACs is to repress the expression of genes that normally does not allow the OPC differentiation, thus liberating the constraints and permitting the differentiation to progress (Swiss et al., 2011). MeCP2 is one of the transcriptional regulators which is expressed throughout the OLG development and is known to play an important role (Nguyen et al., 2013; Sharma et al., 2015). MeCP2 phosphorylation is affected by various extracellular stimuli which inturn affect the functionality of MeCP2 by changing the affinity for its partners and chromatin (Li and Chang 2014). In the present study of oligodendrocytes, we demonstrated that ECM is more important stimuli than other growth factors for regulating pS80MeCP2 phosphorylation. Result shows LN-dependent differential regulation of the pS80MeCP2 in OLG lineage progression. Moreover, on blocking α6β1,the only receptor of LN, in mature OLGs,there was significant increase in pS80MeCP2 levels which suggests that there is LN dependent dephosphorylation in mature OLGs. Next, the chromatin association of pS80MeCP2 in mature OLGS was analyzed using fluorescence microscopy. The data suggests that pS80MeCP2 is in close association with chromatin (Fig 5.1). It is well known that eukaryotic genomes are packaged and organized into two major and distinct forms of chromatin i.e. euchromatin and heterochromatin (Horn and

Peterson 2006). These can be distinguished by differences in DNA composition, histone modifications and associated chromosomal proteins. Heterochromatin is condensed, transcriptionally inert and displays low levels of recombination whereas euchromatin is decondensed, transcriptionally active and replicates relatively early during the cell cycle (Moazed 2001; Richards 2002; Milot et al., 1996). Heterochromatin plays important roles in the maintenance of chromosome integrity and in regulating gene expression in eukaryotes (Weiler and Wakimoto 1995; Grunstein 1998). Moreover, data from the present study confirmed that LN enhanced the expression of MBP in mature OLGs (chapter 4). Earlier studies from our laboratory have shown that MeCP2 regulates MBP expression in OLGs (Sharma et al. 2015). Data from the present study shows that LN regulates both MBP and MeCP2 phosphorylation at S80 site. Hence, results indicate that pS80MeCP2may be a link between LN-dependent MBP expressions. The data from the present study along with others have shown the regulation of myelin proteins by MeCP2 (Ballas et al. 2009; Nguyen et al. 2013; Sharma et al. 2015). Therefore, results suggest that LN-dependent phosphorylation dynamics of MeCP2 may play a critical role in the gene regulation during OLG development. These observations are the first evidence thatMeCP2 is phosphorylated in a stimulus-dependent manner during oligodendrocyte development, and thereby, it may further regulate the oligodendrocyte behavior. Overall, the data also pinpoints the importance of ECM is more than GFs in the regulation of MeCP2 phosphorylation at S80 site. However, further effortsto better understand the mechanisms by which S80 phosphorylation regulates MeCP2 function in OLGs may further our understanding of how mutations in MeCP2 lead to the neurological phenotype of RTT. In-depth understanding of the importance of ECM-dependent signaling in epigenetic regulation will help in the development of well-targeted therapies for the pathobiology of RTT.

Post-translational modification of histones, ATP-dependent chromatin remodeling, and DNA methylation are interconnected nuclear mechanisms that ultimately lead to the changes in chromatin structure necessary to carry out epigenetic gene expression control (Cvekla and Duncanc 2007). Cell differentiation is characterized by a specific gene expression profile in association with the acquisition of a defined tissue architecture and function. The elements critical for cellular differentiation, like extracellular stimuli,

adhesion and cell shape properties, and transcription factors all contribute to the modulation of gene expression and thus, are likely to impinge on the nuclear mechanisms of epigenetic gene expression control (Lelièvre 2009). However, how these elements modify chromatin structure in a hierarchical manner by acting on the nuclear machinery is not known.

In the primary culture of astrocytes, it was demonstrated that pS421MeCP2 was up-regulated by the BDNF treatment. Moreover, BDNF also results in the nuclear accumulation of pS421MeCP2. Hence, in this chapter, investigations were done to understand the molecular mechanism underlying the increase in pS421MeCP2 phosphorylation. By blocking CamkII there was significant decrease in the pS421MeCP2 phosphorylation in BDNF treated astrocytes. These observations are in agreement with already published data in neurons where it has been shown that pS421MeCP2 phosphorylation is mediated by the CamkII and it is activity dependent, i.e on depolarization by KCL or neurotrophins pS421MeCP2 is phosphorylated (Zhou et al., 2006). Moreover, data also indicated that there was decline in the levels of pS421MeCP2 in the K252a (inhibitor of TkB receptor) treated group. Earlier, studies have shown that astrocytes predominately express TrkBT1 and respond to brief application of BDNF by releasing calcium from intracellular stores (Rose et al., 2003). Moreover, it is reported that the overexpression of BDNF in hippocampal astrocytes elicited anxiolytic-/antidepressant-like effects either alone or in combination with fluoxetine thereby providing the first in vivo evidence that this cell type might be a key partner of neurons during antidepressant treatment (Quesseveur et al., 2013). Also, it has been reported that BDNF enhances GAT-1-mediated GABA transport in cultured astrocytes (Vaz et al., 2011). This suggests the importance of BDNF in astrocytes. One important study by Djalali et al., 2005 reported that BDNF is required for the local expression of S100b and production of MBP. In addition, it is reported that MeCP2 binds to the highly-methylated regions of genes such as astrocyte-specific GFAP and S100B and suppresses their expression (Cheng et al., 2011; Namihira et al., 2004). Therefore, it is easy to speculate that these genes might be regulated by BDNF dependent MeCP2 pS421 phosphorylation. Furthermore, using fluorescence microscopy, the chromatin association with pS421MeCP2 upon BDNF treatment in astrocytes was also analyzed. The

immunofluorescence imaging showed that pS421MeCP2 is associated with euchromatin upon BDNF treatment. This is in conjunction with the reported studies suggesting that pS421MeCP2 is associated with the active genes.

Next, investigations on molecular mechanisms underlying MeCP2 phosphorylation in C6 glioma cell line following stimulation by BDNF were analyzed. Using the C6 glioma cell line as an astrocyte cell line, one cannot ignore the fact that it is tumorous cell line and this might be one of the reasons for the differential phosphorylation of MeCP2 by BDNF in C6 glioma cell line. It is well known that the over-expression of BDNF/TrkB results into an increased migration of tumor cells and primes cancer cells to resist from significant genotoxic stressors, most of which are front-line chemotherapies (Heinen et al., 2016; Jaboin et al., 2002; Jia et al., 2015). Increasing evidence suggests that BDNF and TrkB over-expression contribute to oncogenesis of human cancers, ranging from neuroblastomas to pancreatic ductal adenocarcinomas, where it may allow tumor expansion and contribute to resistance to antitumour agents (Zhang et al., 2016), representing that this signaling pathway seems to be abundant in the progression of multiple cancers and dynamically regulates several aspects of tumor cell physiology. A recent *in vitro* study in C6 glioma demonstrated that exogenous recombinant mature BDNF increased the C6 glioma growth and decreased the apoptosis. However, the epigenetic mechanisms underlying this are largely unknown. In the present work, it was demonstrated that there is an increase in pS80MeCP2 and pS421MeCP2 when C6 glioma cell line is treated with BDNF and this phosphorylation is mediated by TrkB receptor. Moreover, when the chromatin association studies were done by immunofluorescence and biochemical fractionation of the nuclei, it was observed that pS80MeCP2 on BDNF treatment is found to be associated with heterochromatin on the contrary pS421MeCP2is associated with euchromatin. MeCP2 is present in the highly nuclease accessible SI fraction of different cell types and tissues (Thambirajahet al., 2012) makes it appealing to speculate a particular type of association of phosphoMeCP2s to regions of the chromocenters whose molecular explanation remains a mystery.

In order to adapt from various environmental stimuli, inflammatory response is essential and it has been generally accepted that astrocytes contribute to these inflammatory

immune responses in the CNS. LPS stimulation leads to a large number of rapid post-translational and transcriptional changes in the astrocytes. In this context, understanding the mechanism by which astrocyte plays a role in CNS immune modulation following a variety of infectious or inflammatory insults needs further investigations. There are reports suggesting that in the peripheral nervous system (PNS), MeCP2 S421 phosphorylation was first observed in the superficial dorsal horn neurons in the spinal cord after induction of peripheral joint inflammation (Geranton et al., 2008). Additionally, they also demonstrated that descending controls regulate MeCP2 phosphorylation, known to relieve transcriptional repression by MeCP2, and Zif268 and Fos expression in the rat superficial dorsal horn, after CFA injection into the hind paw. Our study is the first to report that LPS stimulation leads to increase in phosphorylation of the transcriptional regulator MeCP2 at S421 site in the rat derived primary astrocytes. Blocking the signaling pathways activated by LPS stimulation mainly PI3K and ERK1/2 pathways using pharmacological inhibitors decreased the expression levels of pS421MeCP2. There was no change in the expression of pS80MeCP2 expression in the LPS treated astrocytes suggesting that pS80MeCP2 may not play an important role in LPS stimulated astrocytes. In contrast to the pS80MeCP2 localization, pS421MeCP2 was found to be localized in cytoplasm compared to the control. Therefore, pS421MeCP2 might play a role in cytoplasm in the reactive astrocytes. Many in vitro experiments have demonstrated that the ERK1/2 signaling pathway contributes to the inflammatory response in astrocytes that is induced upon stimulation with LPS (Park et al., 2009; Fields et al., 2013). Studies have shown that when ERK1/2 pathway is blocked by using various pharmaceutical-based therapies it leads to reduction in neuroinflammation in stroke, neurodegenerative disorders, intracranial infections and many other diseases (Wang et al., 2010; Shao et al., 2013; Zhao et al., 2013; Xia et al., 2015). Furthermore, the accumulating evidence indicates that ERK1/2 also takes part in regulating the proliferation and differentiation of astrocytes in the developing brain thereby providing an insight into the mechanisms involved in ERK1/2-mediated regulation of normal and abnormal astrocyte function during brain development.ERK1/2 are involved in LPS signaling in astrocytes (Gorina et al., 2010). The same group suggested that the inhibition of pERK1/2 withU0126 reduced the expression of Egr-1.

Interestingly, Egr-1 gene is a target of MeCP2 reported in astrocytes. Therefore, we speculate that LPS mediated MeCP2 phosphorylation may control the gene expression of Egr-1 gene in astrocytes. Maezawaet al. 2009 has shown that MeCP2 deficiency progressively spreads between MeCP2-deficient and wild-type astrocytes via gap junctions. Considering the increased cytoplasmic distribution of pS421MeCP2 after the LPS stimulation in astrocytes, these amplified levels of pS421MeCP2 may act as messengers between astrocytes involved in the spread of MeCP2 deficiency.

In conclusion, our study provides evidence for the first time that MeCP2 phosphorylation is regulated by extracellular stimuli in glial cell types and distinct signaling pathways are involved in the stimuli mediated MeCP2 phosphorylation. Our findings raise a possibility thatpS80MeCP2 and pS421MeCP2may play an important role in glial cell function (oligodendrocytes and astrocytes) regulated by different extracellular stimuli (LN, BDNF, LPS) by changing its sub-cellular localization and chromatin association. This study may provide further insights into glial contribution to the pathology of RTT.

Fig 5.1

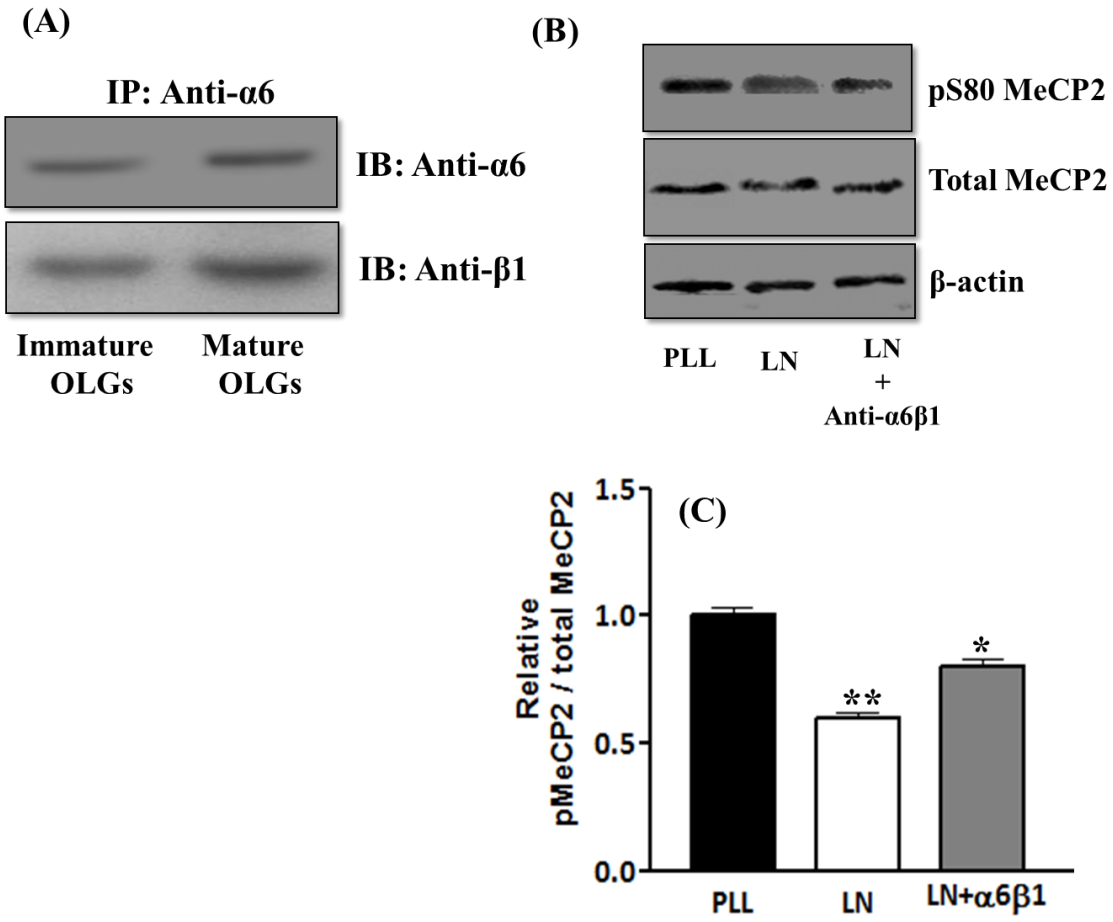
(A)
IP: Anti-α6
IB: Anti-α6
IB: Anti-β1
Immature OLGs
Mature OLGs
(B)
pS80 MeCP2
Total MeCP2
β-actin
PLL
LN
LN + Anti-α6β1
(C)
Relative pMeCP2 / total MeCP2
1.5
1.0
0.5
0.0
**
*
PLL
LN
LN+α6β1

Fig. 5.1(D)

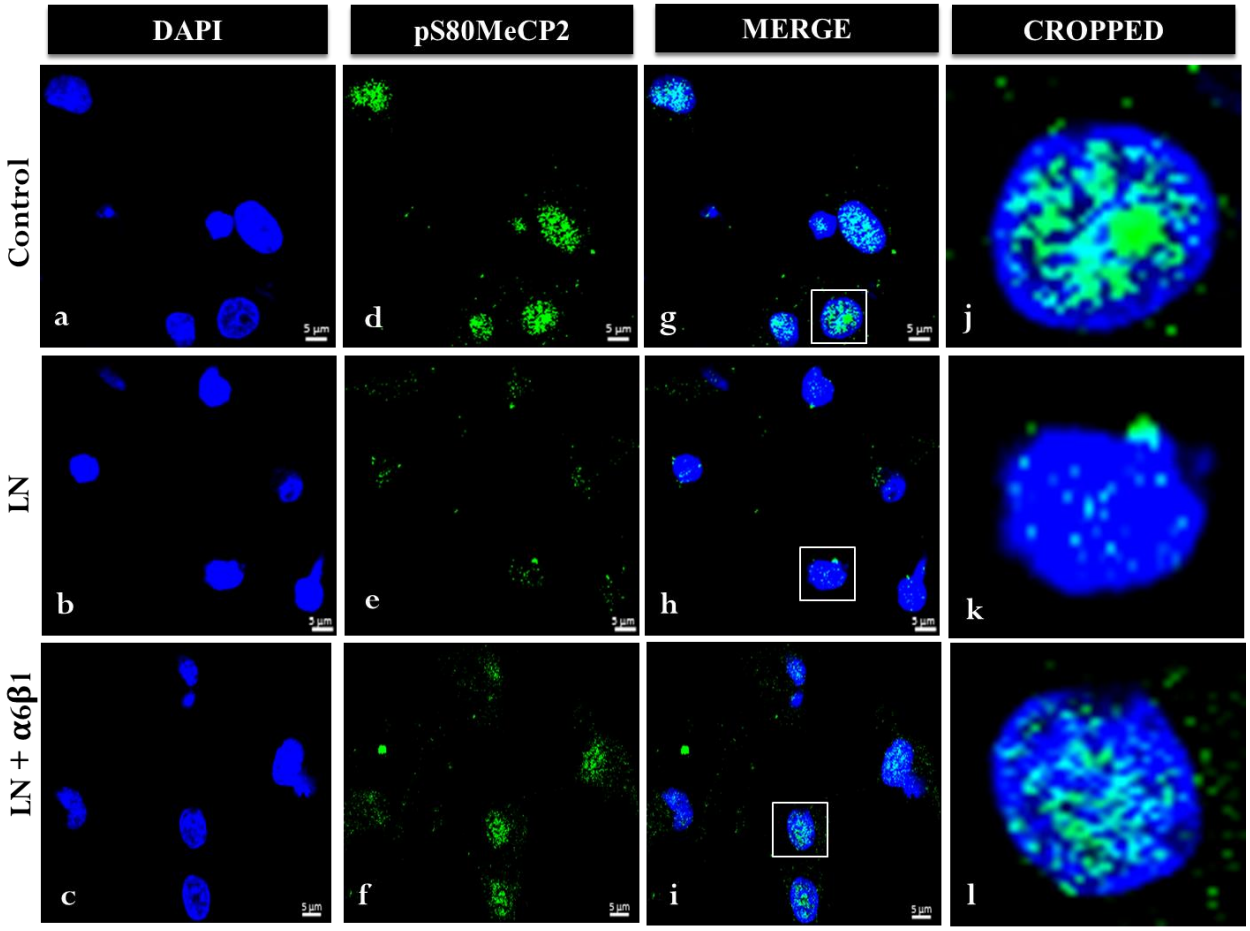
DAPI
pS80MeCP2
MERGE
CROPPED
Control
LN
LN + α6β1
a
b
c
d
e
f
g
h
i
j
k
l
5 µm

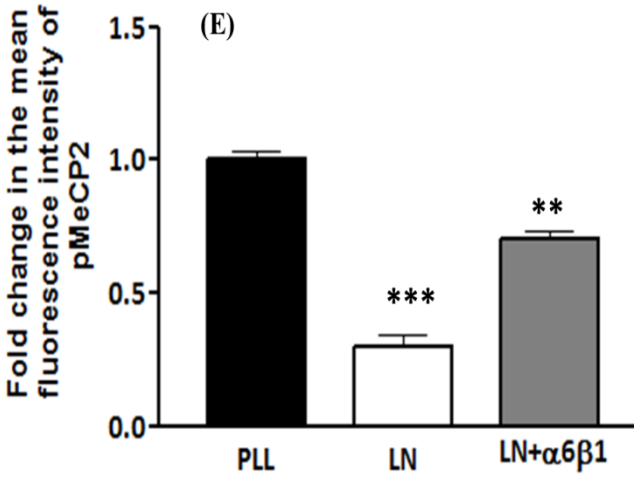
(E)
Fold change in the mean fluorescence intensity of pMeCP2
1.5
1.0
0.5
0.0
***
**
PLL
LN
LN+α6β1

Fig 5.1 α6β1-Integrin mediates the LN dependent dephosphorylation of MeCP2 at S80 in OLGs *(A) Expression of α6β1 integrin in immature and mature OLGs. Cell lysates from immature and mature OLGs were incubated with α6 antibody. After immunoprecipitation, proteins were separated by SDS-PAGE under the non-reducing conditions and immunoblotted with indicated anti-α6 and anti-β1 antibodies. IP:immunoprecipitation, IB:immunoblot. (B) Representative Western blot for phosphorylated (MeCP2 S80) and total MeCP2 in mature OLGs exposed to PLL control, LN, and anti- α6β1 integrin antibody. (C) Graph shows increased levels of pS80MeCP2 in anti-α6β1 integrin antibody-treated group. (D) Immunocytochemistry showing anti-α6β1 integrin antibody increases the pS80MeCP2 expression in LN treated OLGs. Representative immunostaining images showing pS80MeCP2 expression in OLGs (green; d–f). The nucleus was stained with DAPI (blue; a–c). Colocalization of pS80MeCP2 and DAPI shown in merge images (g–i). (j–l) are cropped images of (g–i). Scale bar= 5μm. (E) Graph shows increased levels of pS80MeCP2 in α6β1 integrin blocking group. Values represent mean ± SEM. Statistical differences between the stimulated and control samples were determined using Student's t test or one-way ANOVA parameter where appropriate (*P < 0.05, **P < 0.01, ***P < 0.001)*

Fig 5.2

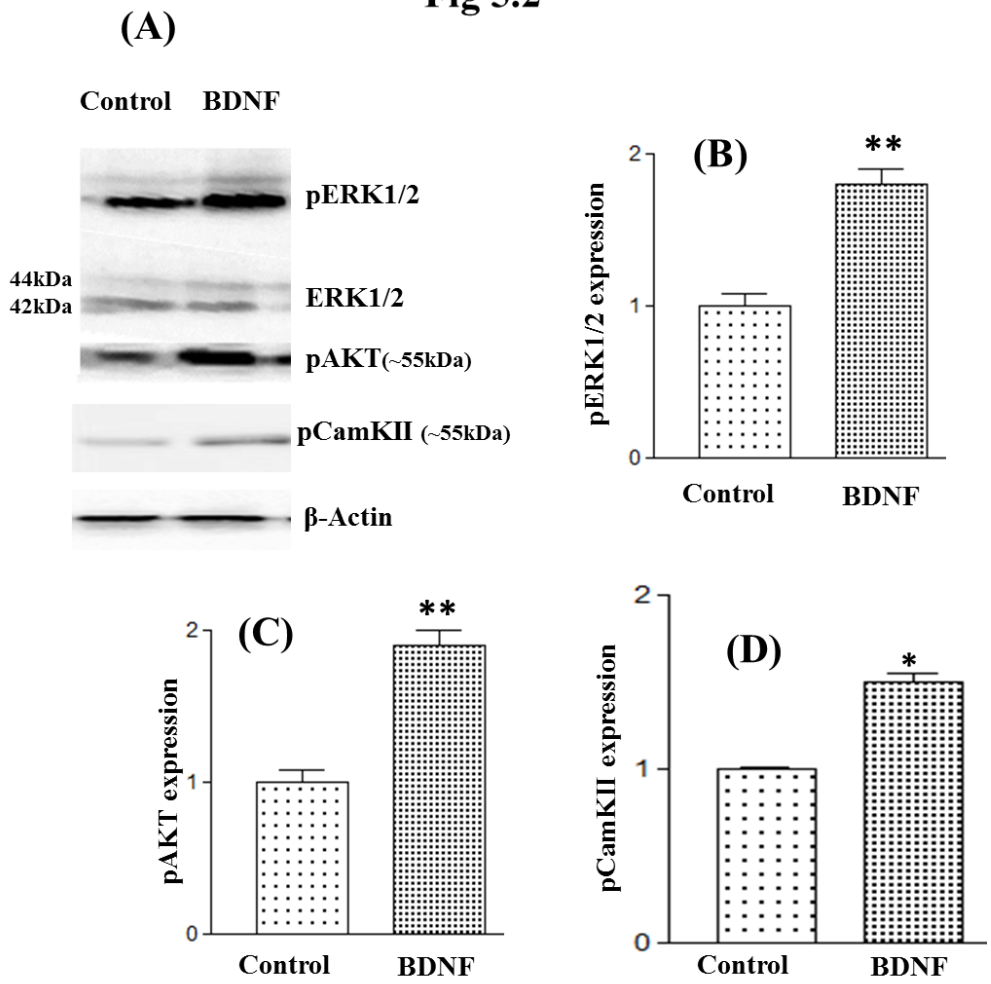
(A)
Control
BDNF
pERK1/2
44kDa
42kDa
ERK1/2
pAKT(~55kDa)
pCamKII (~55kDa)
β-Actin
(B)
**
pERK1/2 expression
2
1
0
Control
BDNF
(C)
**
pAKT expression
2
1
0
Control
BDNF
(D)
*
pCamKII expression
2
1
0
Control
BDNF

Fig 5.2

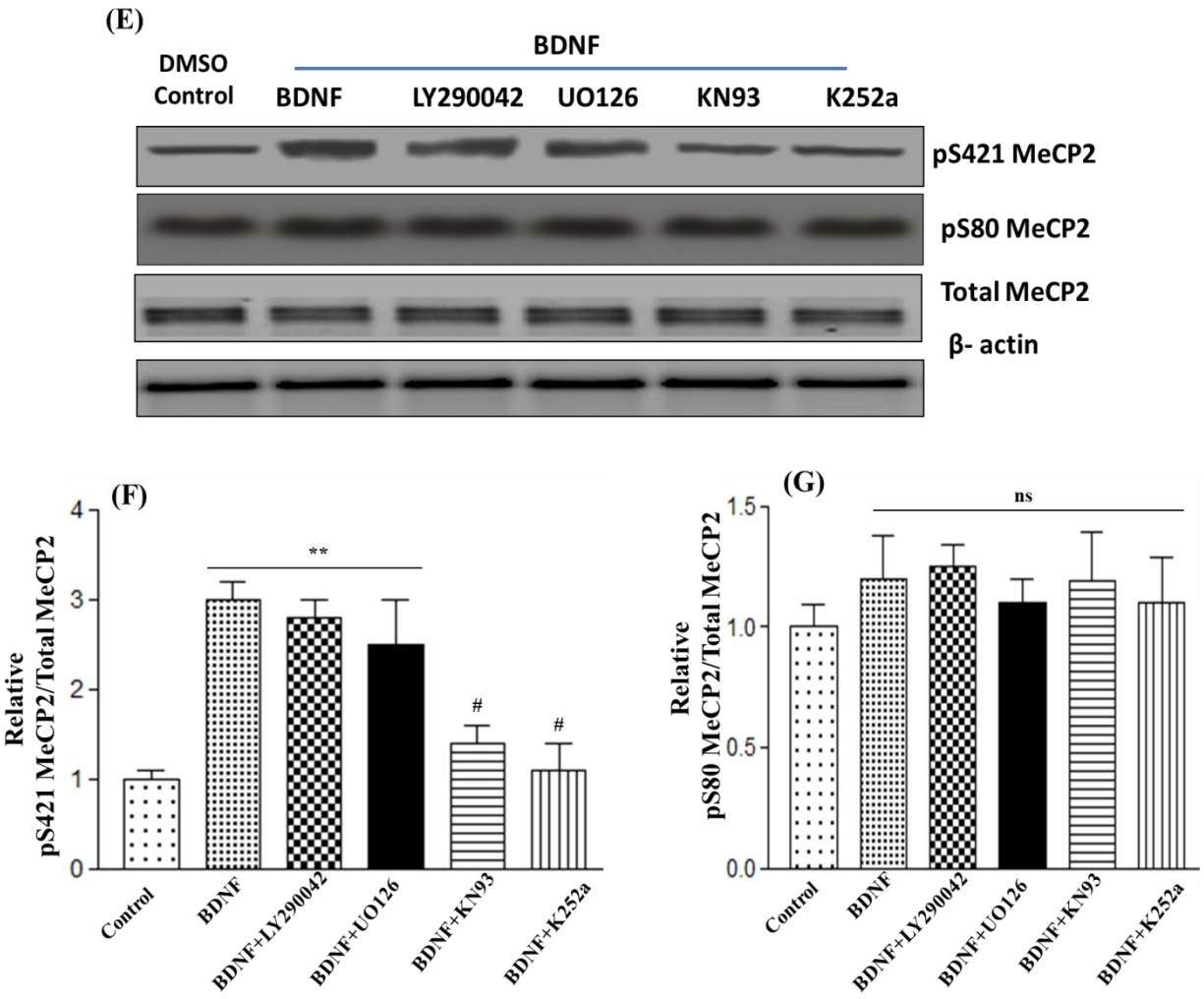
(E)
DMSO Control
BDNF
BDNF
LY290042
UO126
KN93
K252a
pS421 MeCP2
pS80 MeCP2
Total MeCP2
β- actin
(F)
Relative pS421 MeCP2/Total MeCP2
**
#
#
Control
BDNF
BDNF+LY290042
BDNF+UO126
BDNF+KN93
BDNF+K252a
(G)
Relative pS80 MeCP2/Total MeCP2
ns
Control
BDNF
BDNF+LY290042
BDNF+UO126
BDNF+KN93
BDNF+K252a

Fig 5.2 CamKII mediates the BDNF dependent phosphorylation of MeCP2 at S421 in Astrocytes *(A) Pathways activated after BDNF treatment in astrocytes. Representative western blot showing the expression of pERK1/2, pAKT and pCamkII in the BDNF treated astrocytes and control groups. (B) Graph shows increased levels of pERK1/2 in the BDNF treated group compared to control. (C) Graph shows increased levels of pAkt in the BDNF treated group compared to control. (E) BDNF-dependent upregulation of MeCP2 S421 phosphorylation is likely mediated by CaMKII. Western blot analysis of whole-cell extracts prepared from astrocytes that were treated with indicated pharmacological inhibitors for 1hr followed by BDNF treatment for 60 min. K252a is an inhibitor of the BDNF receptor TrkB. (F) Graph shows decreased levels of pS421MeCP2 in KN93 inhibitor group and K252a group compared to BDNF treated group. (G) Graph shows no significant difference in the levels of pS80MeCP2 in the BDNF treated and the inhibitors group. Three different cell preparations were analyzed three times N= 3. Values represent mean ± SEM. Statistical differences between the stimulated and control samples were determined using Student's t test or one-way ANOVA parameter where appropriate. (Treatments compared to control *P<0.05, **P<0.01, ***P<0.001, ns= non-significant). (Treatments compared to BDNF treated group $^{\#}P<0.05$, $^{\#\#}P<0.01$, $^{\#\#\#}P<0.001$, ns= non-significant)*

Fig 5.3

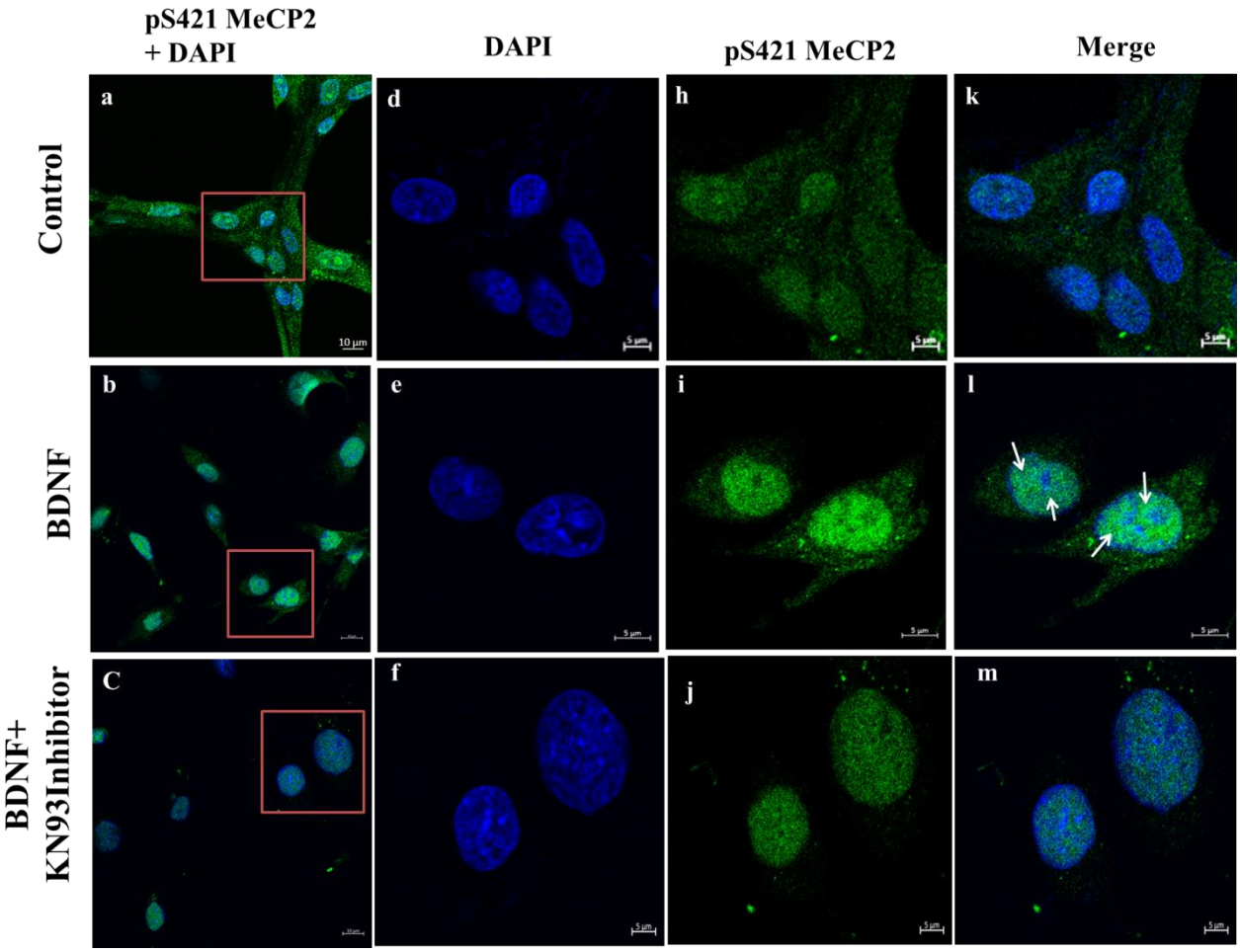

Fig 5.3 Cam KII mediates the BDNF dependent phosphorylation of pS421MeCP2 association with chromatin in Astrocytes *(A) Immunocytochemistry showing KN93 inhibitor decreases the pS421MeCP2 expression in BDNF treated astrocytes (a-c). Magnification of the region indicated by boxes showing pS421MeCP2 expression in (green; g–i). The nucleus was stained with DAPI (blue; d–f). Colocalization of pS421MeCP2 and DAPI shown in merge images (j–l) are cropped images of (g–i). Scale bar= 5µm.*

Fig 5.4

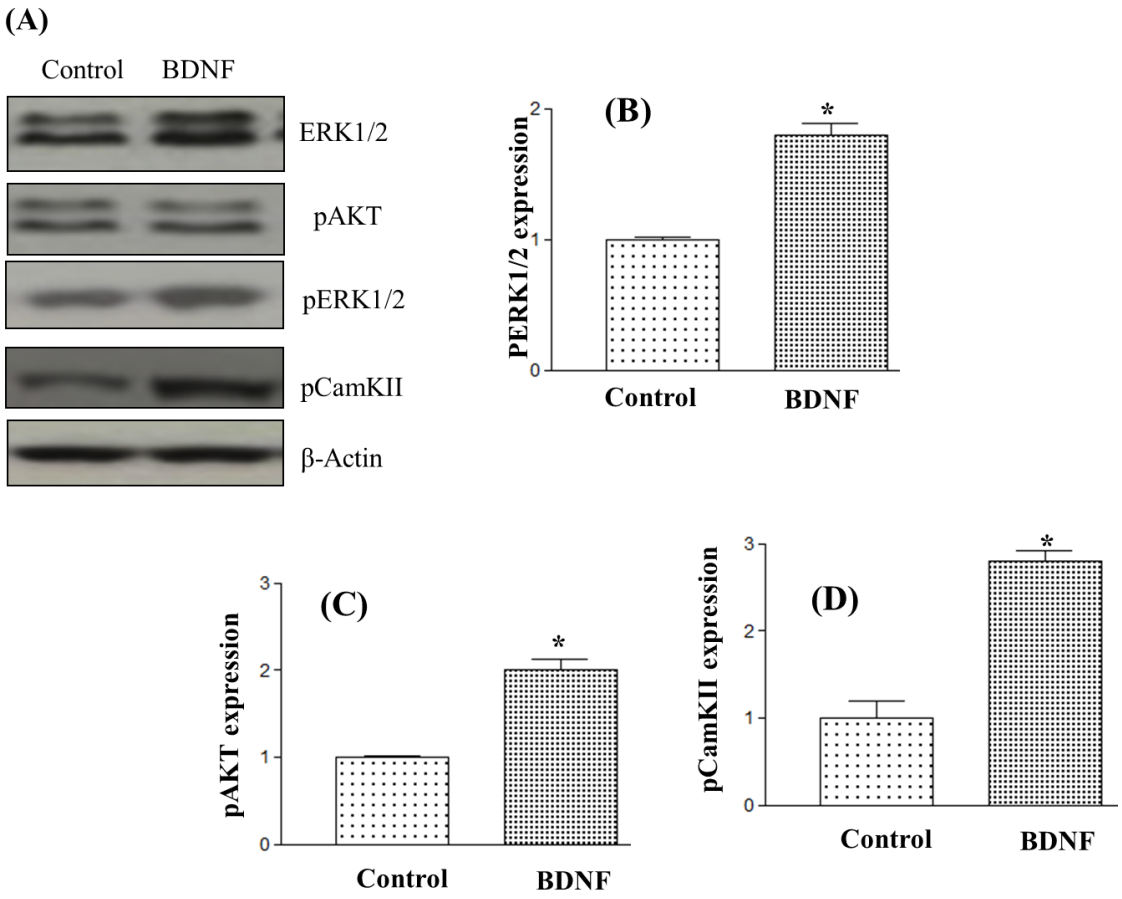
(A)
Control
BDNF
ERK1/2
pAKT
pERK1/2
pCamKII
β-Actin
(B)
PERK1/2 expression
Control
BDNF
(C)
pAKT expression
Control
BDNF
(D)
pCamKII expression
Control
BDNF

Fig 5.4

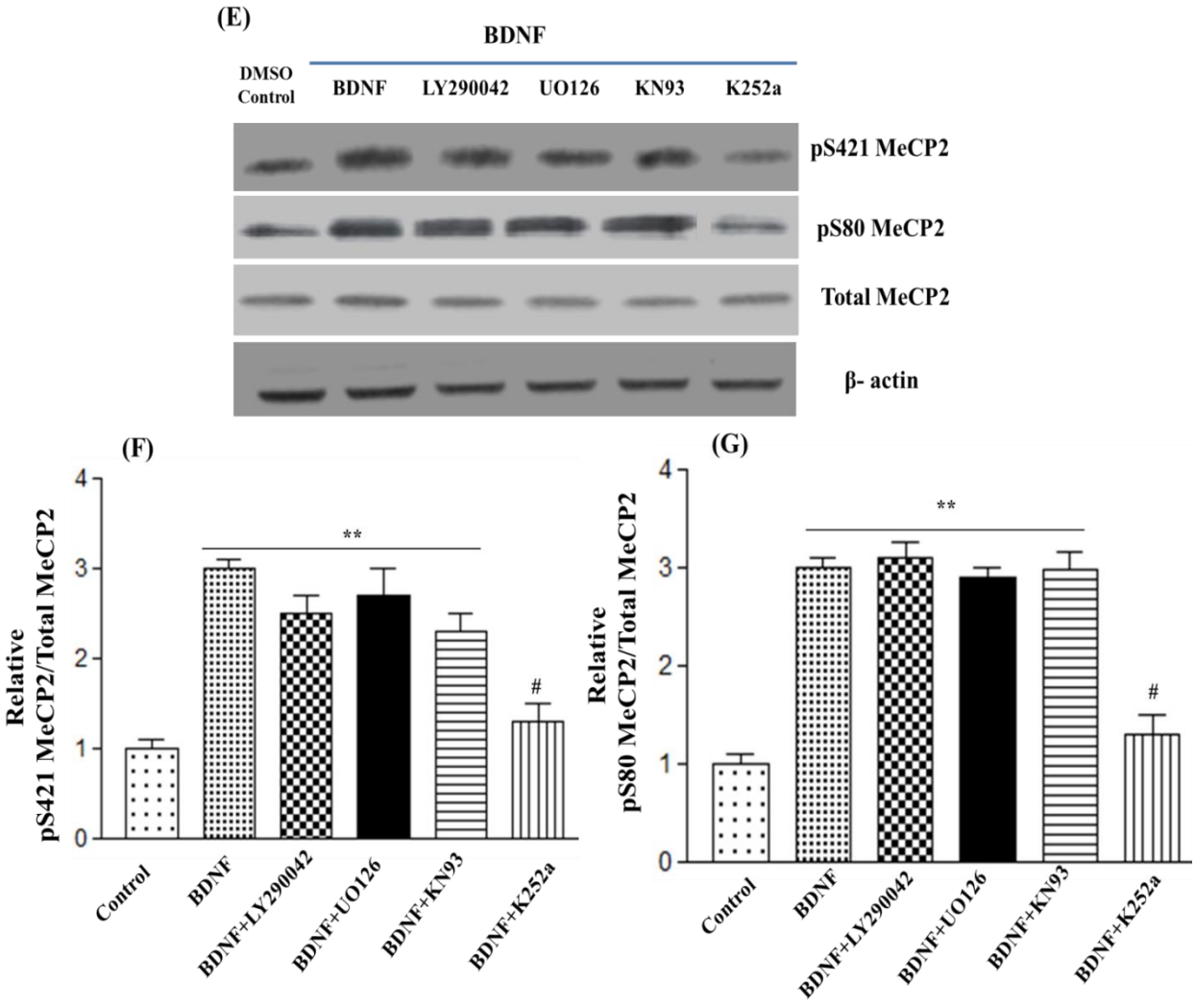
(E)
BDNF
DMSO Control
BDNF
LY290042
UO126
KN93
K252a
pS421 MeCP2
pS80 MeCP2
Total MeCP2
β- actin
(F)
Relative pS421 MeCP2/Total MeCP2
**
#
Control
BDNF
BDNF+LY290042
BDNF+UO126
BDNF+KN93
BDNF+K252a
(G)
Relative pS80 MeCP2/Total MeCP2
**
#
Control
BDNF
BDNF+LY290042
BDNF+UO126
BDNF+KN93
BDNF+K252a

Fig 5.4 BDNF differentially regulates pMeCP2S80 and pMeCP2S421 expression in C6 glioma *(A) Pathways activated after BDNF treatment in C6 glioma. Representative western blot showing the expression of pERK1/2, pAKT and pCamkII in the BDNF treated C6 glioma. (B) Graph shows increased levels of pERK1/2 in the BDNF treated group compared to control. (C) Graph shows increased levels of pAkt in the BDNF treated group compared to control. (D) Graph shows increased levels of pCamKII in the BDNF treated group compared to control. (E) BDNF-dependent upregulation of MeCP2 S421 and MeCP2 S80 phosphorylation is likely mediated by TrkB. Western blot analysis of whole-cell extracts prepared from astrocytes that were treated with indicated pharmacological inhibitors for 1hr followed by BDNF treatment for 60 min. K252a is an inhibitor of the BDNF receptor TrkB. (F) Graph shows decreased levels of pS421MeCP2 in K252a inhibitor group compared to BDNF treated group. (G) Graph shows substantial decrease in the levels of pS80MeCP2 in the K252 inhibitor group compared to BDNF treated group. Three different cell preparations were analyzed three times N= 3. Values represent mean ± SEM. Statistical differences between the stimulated and control samples were determined using Student's t test or one-way ANOVA parameter where appropriate. (Treatments compared to control *P<0.05, **P<0.01, ***P<0.001, ns= non-significant). (Treatments compared to BDNF $^{\#}$P<0.05, $^{\#\#}$ P<0.01, $^{\#\#\#}$ P<0.001, ns= non-significant)*

Fig 5.5 (A)

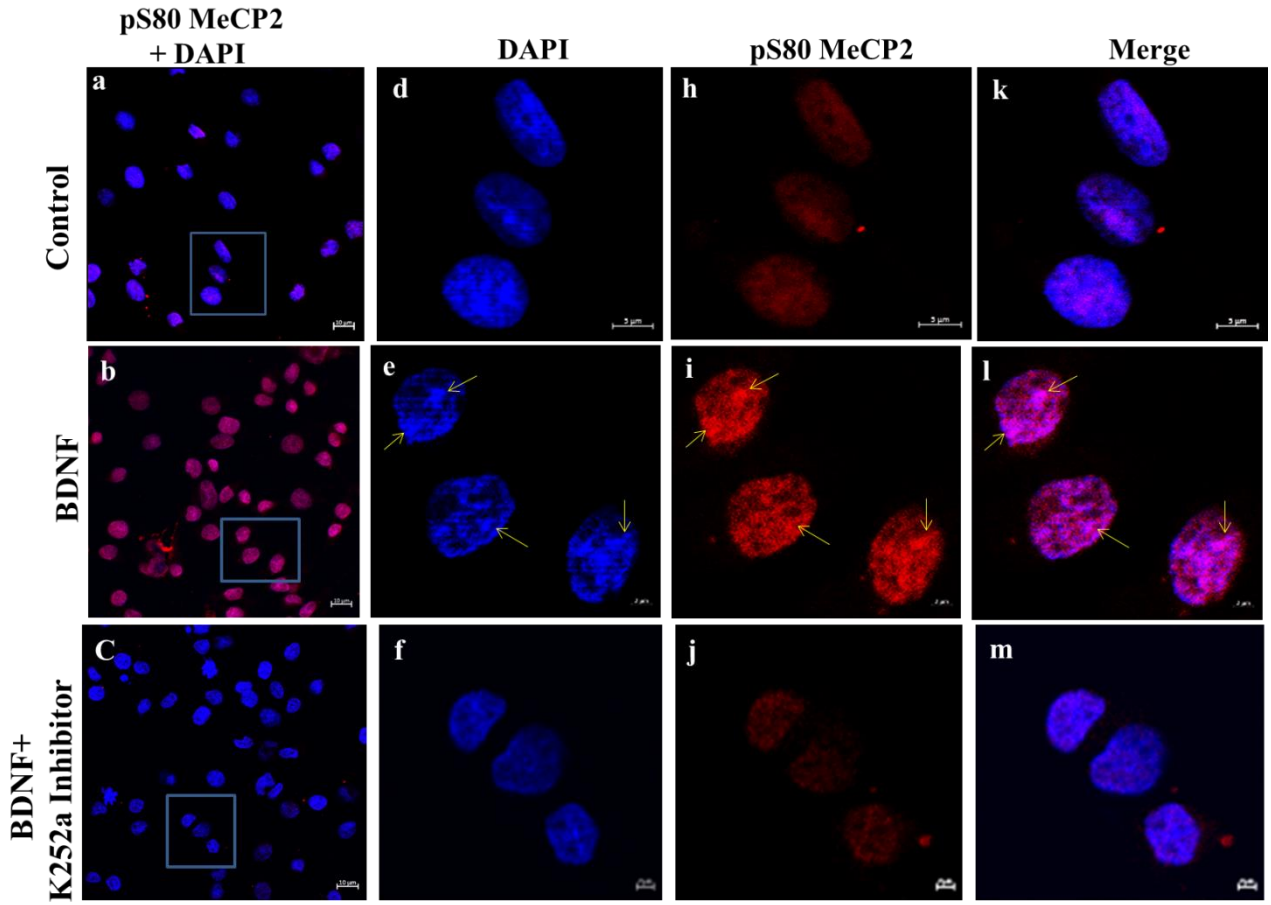
pS80 MeCP2 + DAPI
DAPI
pS80 MeCP2
Merge
Control
BDNF
BDNF+ K252a Inhibitor
a
b
C
d
e
f
h
i
j
k
l
m

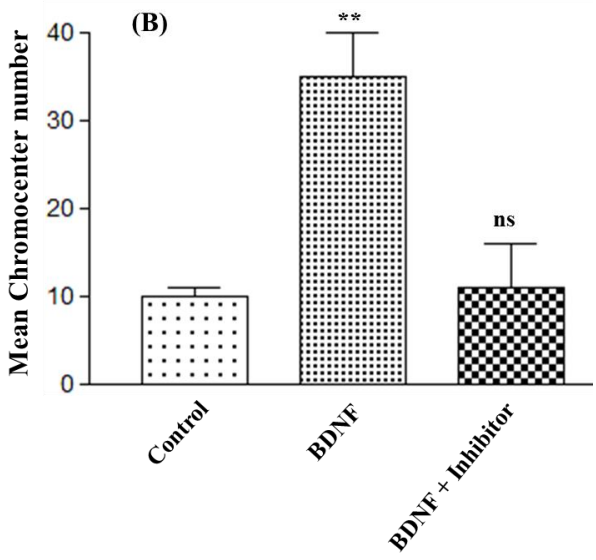
(B)
Mean Chromocenter number
40
30
20
10
0
**
ns
Control
BDNF
BDNF + Inhibitor

Fig 5.5 (C)

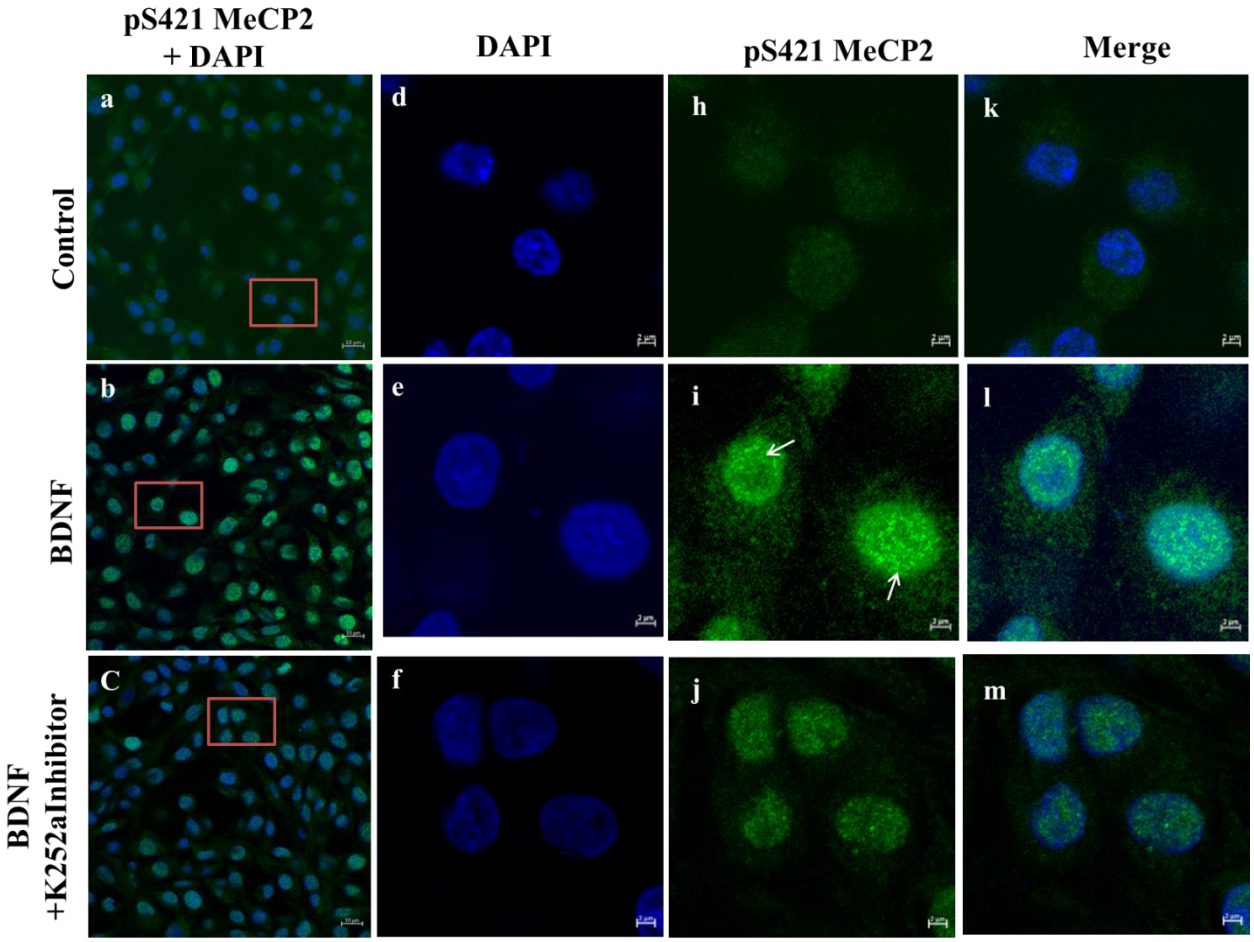

Fig 5.5 BDNF treatment lead to differential sub-nuclear distribution of phospho-MeCP2s in C6 glioma.. *(A) Immunofluorescent staining of the pMeCP2S80 in the BDNF treated C6 glioma with or without K252a inhibitor. DAPI was used to visualize heterochromatic foci (chromocenters). Bar, 10μm. Magnification of the region indicated by boxes in red box containing a heterochromatic chromocenter. (d-f) are the DAPI stained nuclei of the indicated boxes of (a-c), (h-j) are the pS80MeCP2 of the nuclei of (a-c) and (k-m) are the merge images. Bar, 2μm. (B) (C) The bar graph shows mean numbers of chromocenters in the control and treated groups of the cells expressing the pMeCP2S80. Graph shows increased levels of pS80MeCP2 associated with chromocenters in BDNF group compared to control. Values represent mean ± SEM. Statistical differences between the stimulated and control samples were determined using*

*Student's t test or one-way ANOVA parameter where appropriate (*P < 0.05, **P < 0.01, ***P < 0.001).(C) Immunofluorescent staining of the pMeCP2S421 in the BDNF treated C6 glioma with or without K252a inhibitor. DAPI was used to visualize heterochromatic foci (chromocenters). Bar, 10µm. Magnification of the region indicated by boxes in red box containing a heterochromatic chromocenter. (d-f) are the DAPI stained nuclei of the indicated boxes of (a-c), (h-j) are the pS421MeCP2 of the nuclei of (a-c) and (k-m) are the merge images. Bar, 5µm.*

Fig 5.6

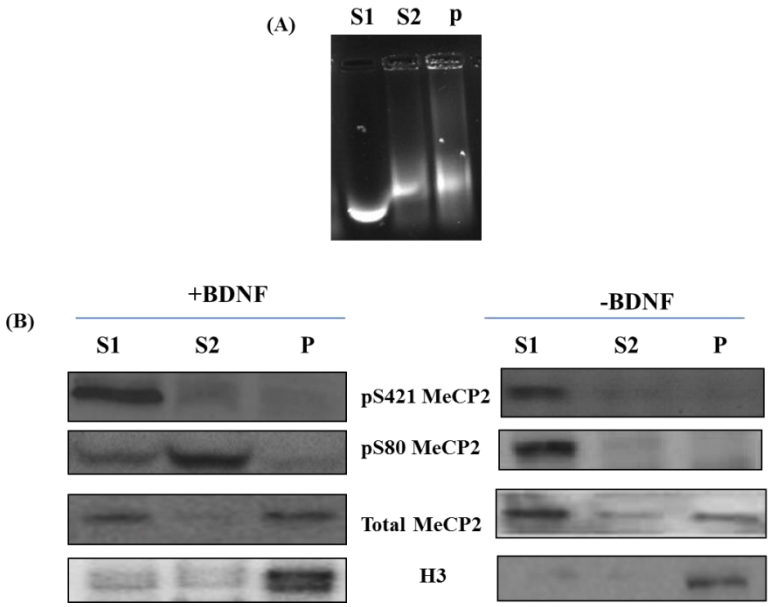

Fig 5.6 BDNF treatment affects the binding of phospho MeCP2s to chromatin. *(A) Gel electrophoresis of DNA from MNase fractions from C6 nuclei. (B) Western blot analysis of MNase fractions from C6 glioma nuclei with or without BDNF treatment with antibodies against pS421MeCP2, pS80MeCP2, total MeCP2 and H3.*

Fig 5.7

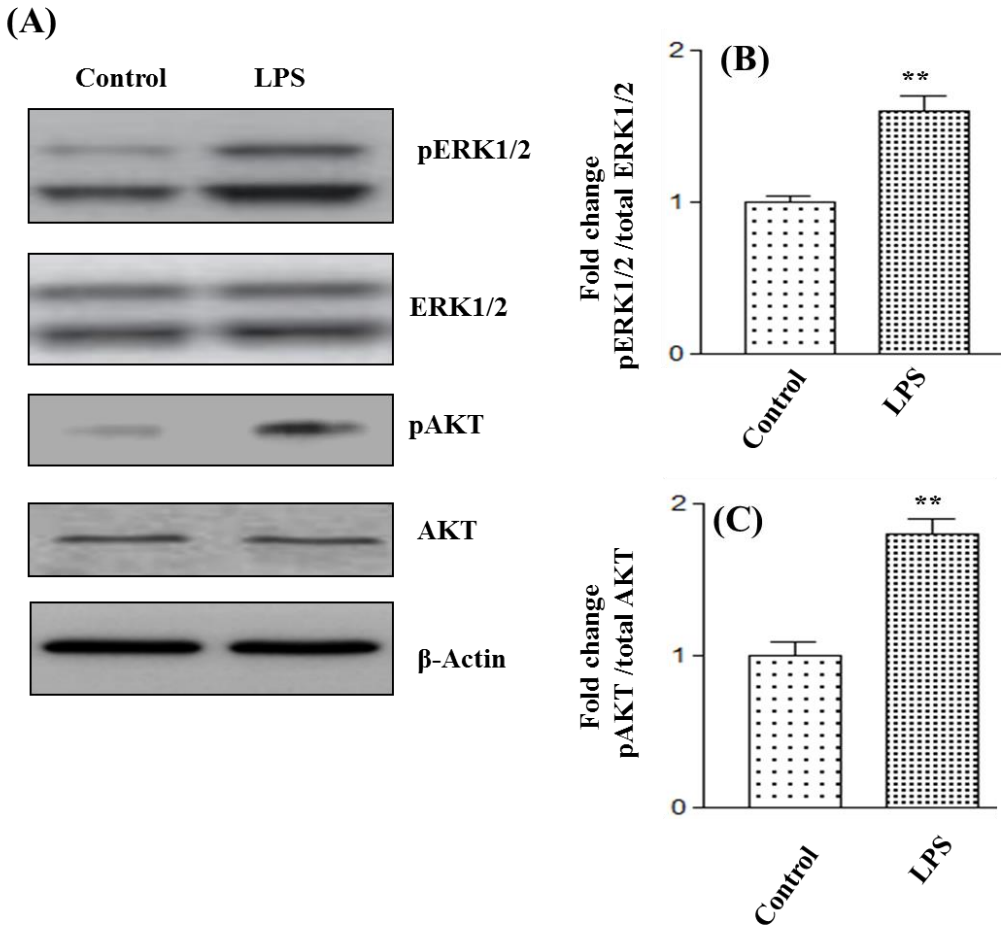
(A)
Control
LPS
pERK1/2
ERK1/2
pAKT
AKT
β-Actin
(B)
Fold change pERK1/2 /total ERK1/2
2
1
0
**
Control
LPS
(C)
Fold change pAKT /total AKT
2
1
0
**
Control
LPS

Fig 5.7

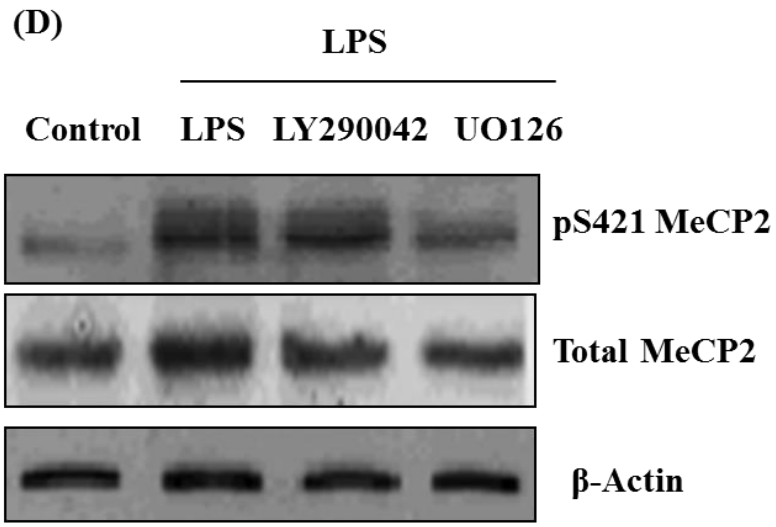
(D)
LPS
Control
LPS
LY290042
UO126
pS421 MeCP2
Total MeCP2
β-Actin

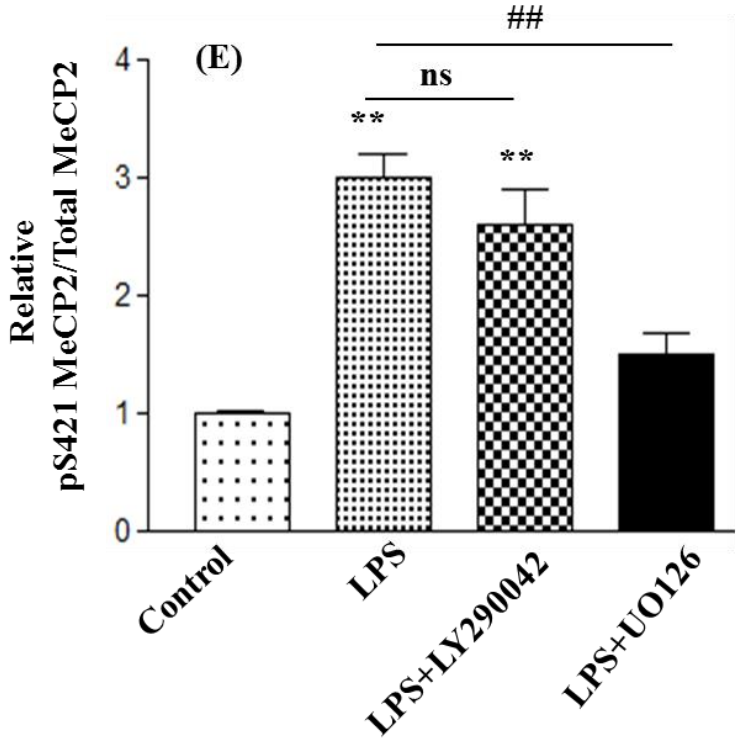
(E)
##
ns
**
**
Relative pS421 MeCP2/Total MeCP2
0
1
2
3
4
Control
LPS
LPS+LY290042
LPS+UO126

Fi g. 5.7(F)

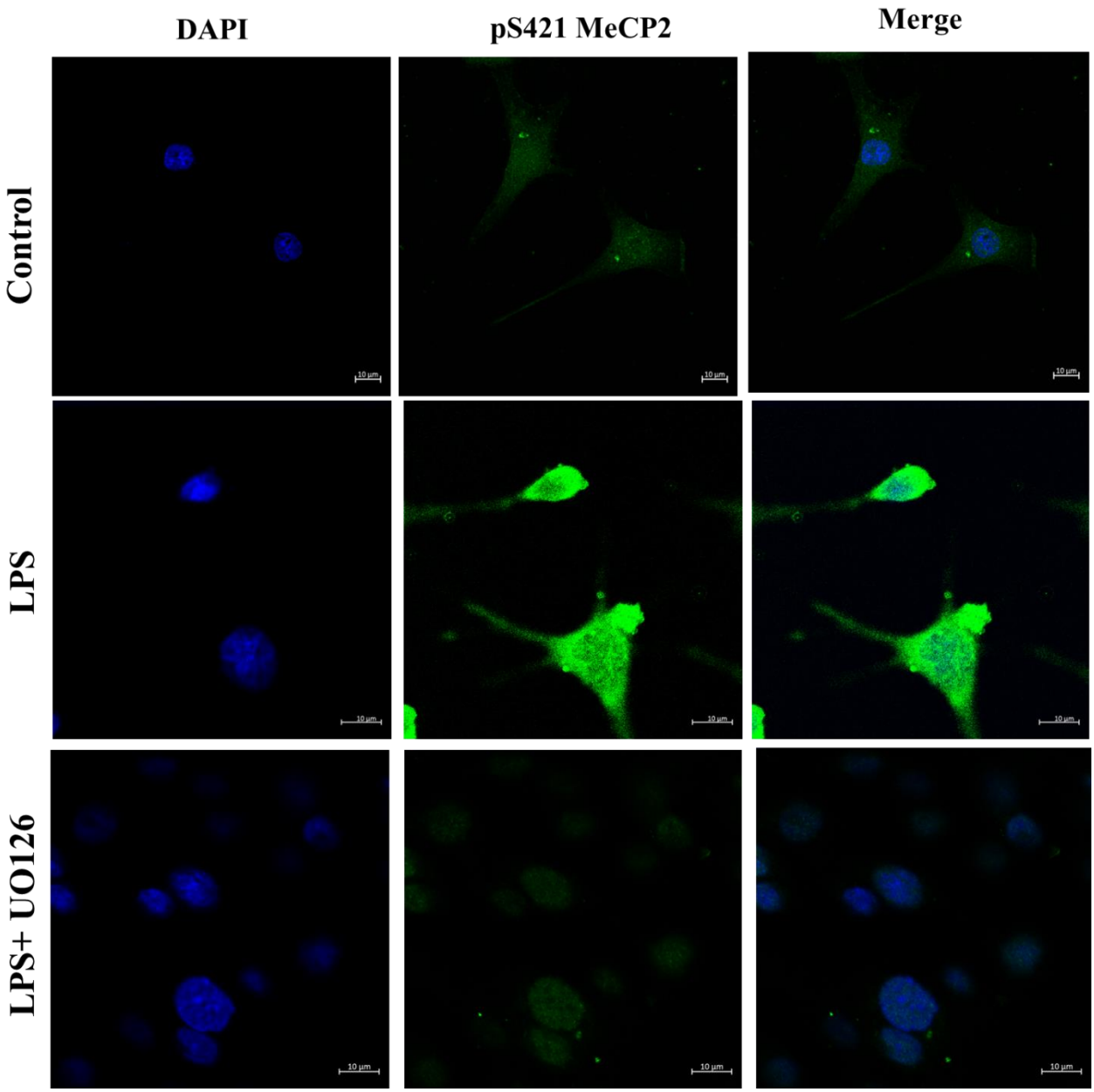

Fig. 5.7 pERK1/2 mediated LPS induced MeCP2 phosphorylation at S421 in Astrocytes *(A) Pathways activated after LPS treatment in astrocytes. Representative western blot showing the expression of pERK1/2 and pAKT in the LPS treated astrocytes and control groups. (B) Graph shows increased levels of pERK1/2in the LPS treated group compared to control. (C) Graph shows increased levels of pAKT in the LPS treated group compared to control. (D) LPS-dependent upregulation of MeCP2 S421 phosphorylation is likely mediated by pERK1/2. Western blot analysis of whole-cell extracts prepared from astrocytes that were treated with UO126 (pharmacological inhibitor of pERK1/2) and LY290042 (pharmacological inhibitor of pAKT) for 60 min followed by LPS treatment for 4hrs. (E) Graph shows decreased levels of pS421MeCP2 in UO126 inhibitor group compared to LPS treated group. (F) Sub-cellular localization of pS421MeCP2 in Astrocytes. Confocal images of immunofluorescent double staining of pS421MeCP2 (green) with DAPI (blue) in the Control, LPS and LPS+UO126 treated cortical astrocytes. Scale bars= 10μm. Three different cell preparations were analyzed three times N= 3. Values represent mean ± SEM. Statistical differences between the stimulated and control samples were determined using Student's t test or one-way ANOVA parameter where appropriate. (Treatments compared to control *P<0.05, **P<0.01, ***P<0.001, ns= non-significant). (Treatments compared to LPS $^{\#}$P<0.05, $^{\#\#}$ P<0.01, $^{\#\#\#}$ P<0.001, ns= non-significant)*